Journal of Magnetism and Magnetic Materials 321 (2009) 4108–4114

Contents lists available at ScienceDirect

Journal of Magnetism and Magnetic Materials

journal homepage: www.elsevier.com/locate/jmmm

# Magnetic and magneto-optical studies on $Zn_{1-x}Cr_xTe$ ($x = 0.05$) films grown on glass substrate

D. Soundararajan [a], D. Mangalaraj [b,*], D. Nataraj [a], L. Dorosinskii [c], J. Santoyo-Salazar [d,e], M.J. Riley [f]

[a] Thin Films and Nanomaterials Laboratory, Department of Physics, Bharathiar University, Coimbatore 641 046, India
[b] Department of Nanoscience and Technology, Bharathiar University, Coimbatore 641 046, India
[c] National Institute of Metrology (TUBITAK-UME), P.K. 54, 41470 Gebze–Kocaeli, Turkey
[d] Instituto de Investigaciones en Materiales, Universidad Nacional Autónoma de México, Circuito Exterior s/n. Ciudad Uuniversitaria AP 70-360, México D.F., 04510, México
[e] Institut de Physique et Chimie des Matériaux de Strasbourg, UMR CNRS-ULP-ECPM 7504, 23, rue du Loess, BP 43, 67034 Strasbourg Cedex 2, France
[f] University of Queensland, School of Molecular Microbial Sciences, St Lucia 4072, Australia

ARTICLE INFO

*Article history:*
Received 28 December 2008
Received in revised form
11 June 2009
Available online 15 August 2009

*Keywords:*
ZnTe:Cr film
Magnetic domains
*M* vs. *H* curve
Magneto-optical study

ABSTRACT

$Zn_{1-x}Cr_xTe$ ($x = 0.05$) films were prepared by thermal evaporation onto glass substrates. X-ray diffraction (XRD) was used to determine the crystalline quality of the ZnTe:Cr film. Magnetic force microscopy (MFM) investigation has shown a non-uniform distribution of magnetic domains with an average size of 4 nm at room temperature. SQUID measurements have further shown that the non-uniform distribution of domains does not affect the room temperature ferromagnetism of this material. Electron spin resonance spectroscopy (ESR) was done to determine the Cr valence state in the ZnTe lattice. Magnetic circular dichroism (MCD) analysis was used to confirm the ZnCrTe phase contributing to the ferromagnetic behavior.



## 1. Introduction

Dilute magnetic semiconductors (DMSs) are the solid solutions of semiconductors with some cations replaced by 3d transition-metal ions [1]. To date, various kinds of DMS systems have been investigated to examine the possibility of practical spintronics applications [2,3]. However, the advantage of DMSs could not be utilized because their Curie temperature is below room temperature. A large amount of research has been carried out on the synthesis of novel DMS materials with room temperature ferromagnetism, and which are mostly based on III–V and II–VI compound semiconductors. The 3d transition metals (TMs) such as Fe, Mn and Co doped II–VI compound semiconductors are potential spintronic materials and this is because of high solubility of the TMs in those compound semiconductors. It has been reported that about 10–25 at% of TMs can be doped into II–VI group compound semiconductors [4]. Much fundamental research has been carried out on this type of DMS, and it was found that there is no ferromagnetic behavior even at very low temperature. This is because of the spin glass nature [5]. However it has been recently found that highly p (nitrogen)-doped ZnTe:Mn, which is a II–VI compound semiconductor, can show ferromagnetism up to 3 K [6]. This high-temperature ferromagnetism is due to the mediation of the ferromagnetic ordering between the magnetic ions and the added hole carriers [7].

In recent years, Cr-doped ZnTe films have attracted a great deal of attention as a new class of DMS, since the replacement of Zn with Cr yielded a net ferromagnetic exchange interaction without p type doping [8]. In the case of Cr doping, replacement of the Zn position itself created a hole as well as a source of magnetic impurity [9]. It has been found that Cr-doped ZnTe is a well-known ferromagnetic semiconductor with $T_c$ values much greater than room temperature [10]. The literature on the magnetic properties of epitaxial films of this material is based on using the molecular beam epitaxial (MBE) method to prepare the films [11,12]. Studies have also attempted to determine whether the observed ferromagnetic behavior is from the ZnCrTe phase or from any other possible Cr-related precipitates using magnetic circular dichroism (MCD) spectroscopy. For example, Saito et al., have used MCD on MBE grown $Zn_{1-x}Cr_xTe$ ($x = 0.20$) epitaxial film and found the origin of ferromagnetism as due to the ZnCrTe phase [10,11].

In the present manuscript, we report studies on the structure, magnetic and magneto-optical properties of ZnTe:Cr films on a glass substrate prepared by thermal evaporation. Initially the incorporation of Cr into ZnTe was confirmed by XRD and ESR spectroscopy. The magnetic properties such as magnetic domain observations and magnetic moment measurements were carried out by MFM and SQUID magnetometer, respectively. Finally, the

* Corresponding author. Tel.: +91 422 2425458; fax: +91 422 2422387.
*E-mail addresses:* dmraj800@yahoo.com, devsoundarrajan@gmail.com (D. Mangalaraj).

0304-8853/$ - see front matter © 2009 Elsevier B.V. All rights reserved.
doi:10.1016/j.jmmm.2009.08.012

MCD spectroscopy was used to confirm the origin of the ferromagnetism from the as-prepared film.

## 2. Experimental details

### 2.1. Film preparation

Appropriate weights of high-pure Zn, Te and Cr (Alfa Aeser) metals were taken together in two different quartz ampoules for the preparation of $Zn_{1-x}Cr_xTe$ molten alloys with $x = 0.0$, and 0.05. The ampoules were vacuum sealed at a vacuum of $10^{-5}$ Torr and then they were kept inside a horizontal tube rotating furnace. In case of pure ZnTe, the vacuum sealed ampoule was maintained at 600 °C for 12 h. In the case of ZnTe:Cr, the ampoule was maintained at 1100 °C for 24 h. In both cases, the temperature of the furnace was slowly increased step by step to the required value and after carrying out the reaction at respective time period, the temperature of the zone was then slowly decreased in steps to room temperature. The molten alloys were taken out and crushed into fine powder by grinding in a mortar. The as-obtained ZnTe and ZnTe:Cr were then used for the growth of respective films. For this, the as-prepared ZnTe and ZnTe:Cr compound powders were taken in tungsten dimple source and thermally evaporated onto well-cleaned glass substrates under a vacuum of $4 \times 10^{-5}$ Torr at ambient temperature.

### 2.2. Characterization techniques

Crystallographic analysis was carried out using a X-ray diffractometer [Model—Shimadzu (XRD-6000), $\lambda = 1.5406$ Å] operated in the $2\theta$ scan range of 20–80°. XPS measurements were carried out using an Escalab 220iXL system (VG Scientific Inc.) with a monochromatic Mg Kα X-ray source (1284.6 eV). The XPS instrument accuracy is about 0.1 atomic percentage. The relative atomic percentage of Zn, Te and Cr were obtained by using XPS peak fit software. A scanning probe microscope, SPM, (JEOL JSPM-4210), was

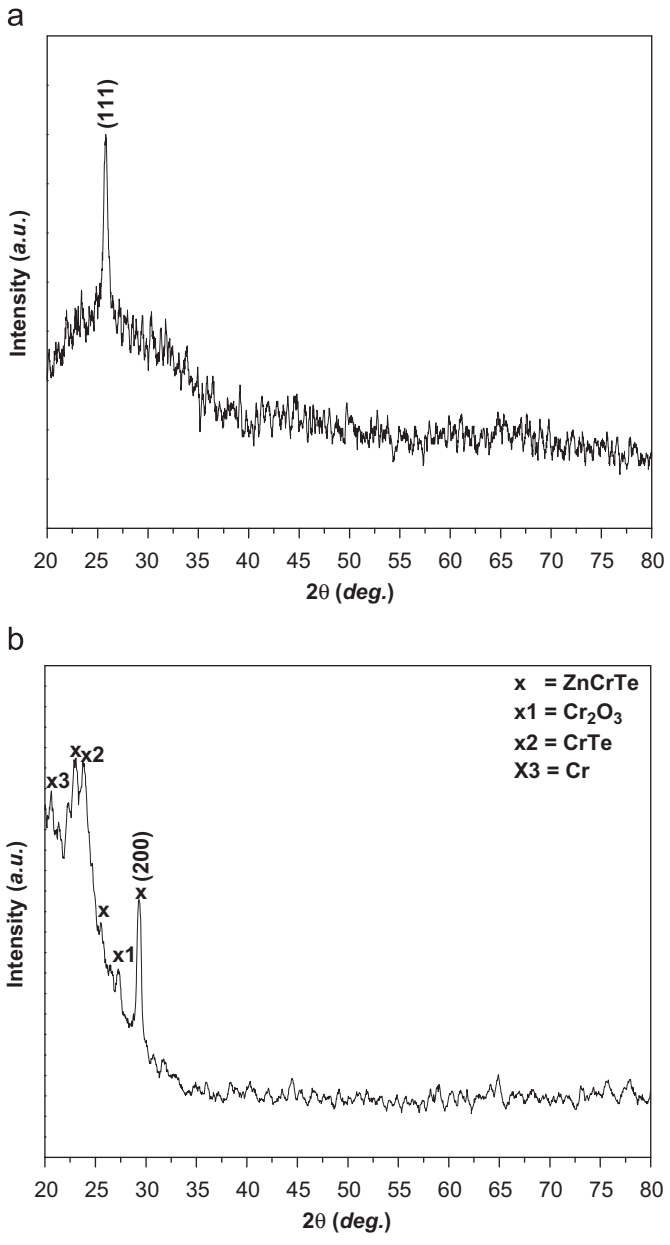


**Fig. 1.** (a and b). X-ray diffraction patterns of (a) ZnTe and (b) ZnTe:Cr films grown on glass substrate.

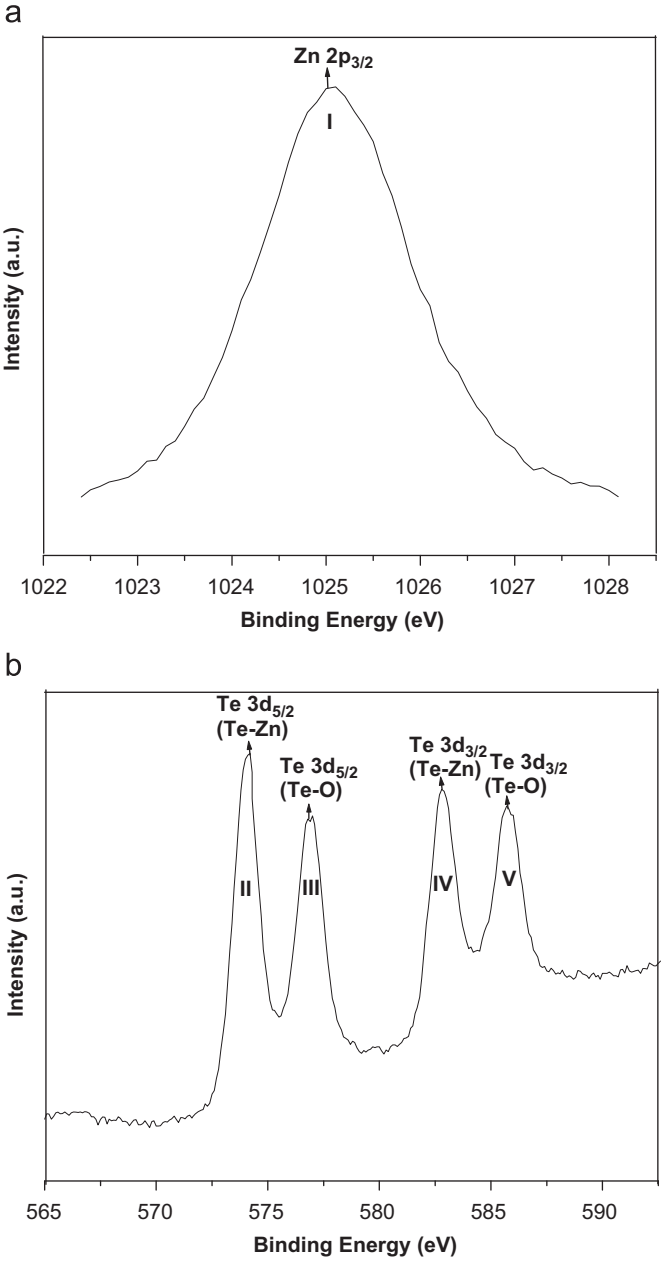


**Fig. 2.** (a and b). High-resolution surface XPS spectra of ZnTe film.

used to measure particle size and magnetic domains at room temperature. Topography of the films was scanned by AFM in Tapping™ mode and magnetic domains were analyzed by MFM in lift mode. For MFM, a magnetic cantilever tip NSC14/Co–Cr of Mikromasch, Co. was used with a resonant frequency of 160 kHz. The 2D and 3D images, profiles, and domains measurements were processed with the software win SPM DPS, JEOL Ltd. Magnetic properties were recorded using a SQUID magnetometer at 300 K. Transmittance mode MCD signals were obtained from a high resolution Jobin Yvon 750s model monochromator with an Oxford Instruments Spectro-Mag superconducting magnet.

## 3. Results and discussion

### 3.1. Structure

The XRD pattern of ZnTe and ZnTe:Cr films are compared and the results are shown in Fig. 1(a and b). The diffraction pattern of the ZnTe film shows a main peak along (1 1 1) crystallographic direction indicating the cubic zinc-blende structure of ZnTe as observed by Akram et al. [13]. In the case of ZnTe:Cr film, poor crystallinity was observed along with a main peak at (2 0 0) crystallographic direction indicating the ZnCrTe cubic zinc-blende structure. This peak is similar to a peak observed by Shinji Kuroda et al. [14,15] for ZnTe:Cr film grown on a GaAs (1 0 0) substrate by the MBE technique. In addition to the main peak along the (2 0 0) crystallographic direction, small peaks were also observed indicating Cr, $Cr_2O_3$ and CrTe precipitates [16,17]. The calculated lattice parameter values of the ZnTe and ZnTe:Cr films are 5.96 and 6.08 Å, respectively. The change in lattice parameter is an indication that Cr has substitutionally incorporated into the ZnTe lattice.

### 3.2. Composition

The microscopic surface composition of the prepared ZnTe and ZnTe:Cr films were investigated by high-resolution XPS. The

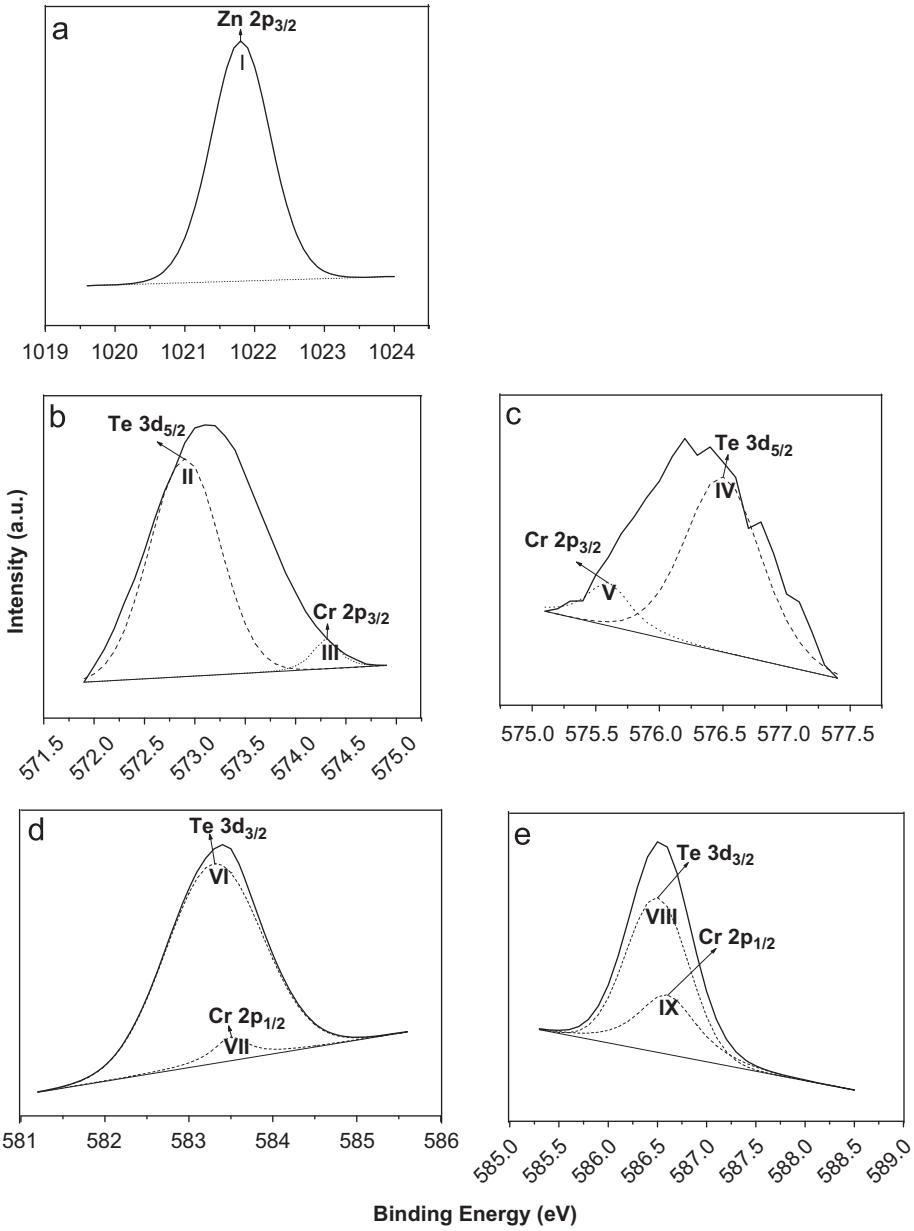


**Fig. 3.** (a–e). High-resolution surface XPS spectra of ZnTe:Cr film.

**Table 1**
Assignments to the component of peaks of the high -resolution surface XPS scans of the ZnTe film.

| Component | Binding energy (eV) | Assignment |
|---|---|---|
| I (Zn $2p_{3/2}$) | 1025.08 | Zn–Te |
| II (Te $3d_{5/2}$) | 574.2 | Te–Zn |
| IV (Te $3d_{5/2}$) | 576.9 | Te–$O_2$ |
| VI (Te $3d_{3/2}$) | 582.9 | Te–Zn |
| VIII (Te $3d_{3/2}$) | 585.7 | Te–$O_2$ |

**Table 2**
Assignments to the component of peaks of the high -resolution surface XPS scans of ZnTe:Cr film.

| Component | Binding Energyenergy (eV) | Assignment |
|---|---|---|
| I (Zn $2p_{3/2}$) | 1021.8 | Zn–Te |
| II (Te $3d_{5/2}$) | 572.9 | Te–Zn |
| III (Cr $2p_{3/2}$) | 574.3 | Cr–Te |
| IV (Te $3d_{5/2}$) | 576.5 | Te–$O_2$ |
| V (Cr $2p_{3/2}$) | 575.6 | $Cr_2$–$O_3$ |
| VI (Te $3d_{3/2}$) | 583.3 | Te–Zn |
| VII (Cr $2p_{1/2}$) | 583.5 | Cr–Te |
| VIII (Te $3d_{3/2}$) | 586.5 | Te–$O_2$ |
| IX (Cr $2p_{1/2}$) | 586.6 | $Cr_2$–$O_3$ |

**Table 3**
Relative atomic percentage of Zn, Te and Cr elements as evaluated from the high -resolution surface XPS spectra of the ZnTe and ZnTe:Cr films.

| Samples | Relative at. % of | | |
|---|---|---|---|
| | Zn | Te | Cr |
| ZnTe | 52.1 | 47.17 | – |
| ZnTe:Cr | 45.0 | 50.03 | 4.97 |

results are shown in Figs. 2(a and b) and 3(a–e). The most probable assignments to the origin of components are presented in Tables 1 and 2 [18]. The relative at% of elements as evaluated from the high-resolution spectra using XPS peak fit software are given in Table 3. Fig. 2(a and b) displays the XPS spectra of ZnTe film and it exhibits the characteristic Zn and Te peak positions. There appeared a single peak for Zn at 1025.08 eV and which corresponds to $2p_{3/2}$ transition. In the case of Te, there appeared two peaks at 574.2 and 582.9 eV and which were corresponds to $3d_{5/2}$ and $3d_{3/2}$ transition, respectively. In addition, in adjacent to these two peaks there appeared another set of peaks at 576.9 and 585.7 eV, which were again corresponds to $3d_{5/2}$ and $3d_{3/2}$ transition but were due to oxide phase of Te (Te–O). A blue shift in the binding energy value of oxide-related peaks suggests a fact that Te has donated electrons to oxygen and therefore the binding energy corresponding to $3d_{5/2}$ and $3d_{3/2}$ transitions has been increased. The stoichiometry of the ZnTe films is determined by using the $2p_{3/2}$ peak for Zn and 3d peaks for Te. The calculated value of relative atomic percentage of Zn and Te contents in ZnTe film is 52.1 and 47.17, respectively. To know the elemental composition, a similar study was also carried out on Cr-doped ZnTe film. Fig. 3(a–e) displays the deconvoluted XPS spectra of ZnTe:Cr film. It shows the characteristic Zn, Te and Cr peaks at their corresponding binding energies. Also, the presence of $TeO_2$ and antiferromagnetic $Cr_2O_3$ components are observed at their corresponding binding energies of 576.5 and 575.6 eV, respectively. The stoichiometry of the ZnTe:Cr film is determined by using the 2p peak for Zn, 3d peaks for Te and 2p peaks for Cr. The estimated value of relative atomic percentage of Zn, Te and Cr contents in ZnTe:Cr film is 45, 50.03 and 4.97, respectively.

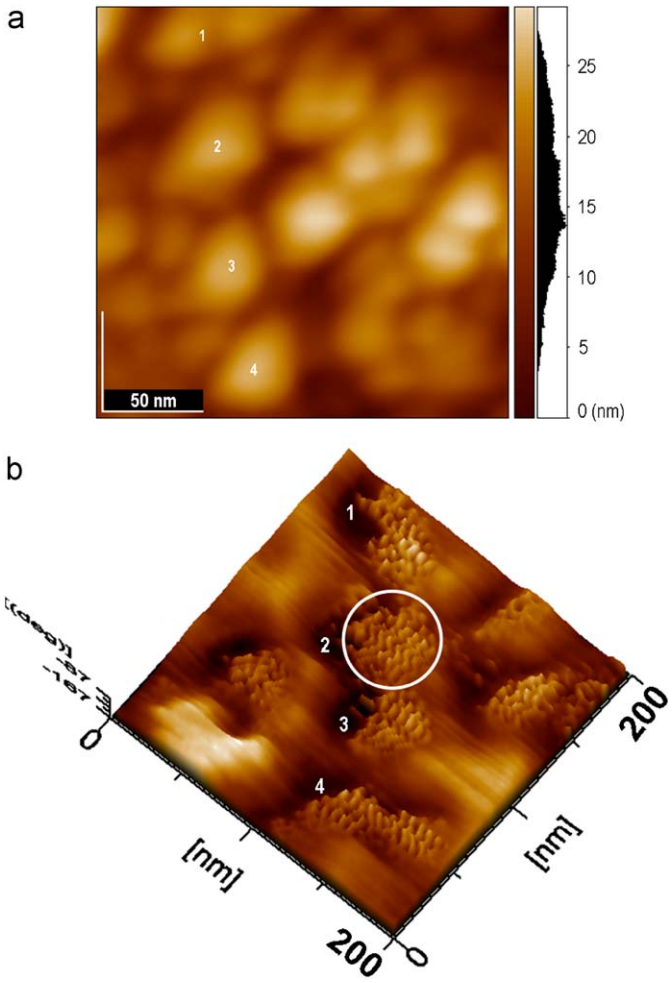


**Fig. 4.** (a and b). AFM and MFM analysis on ZnTe:Cr film grown on glass substrate. (a) Distribution of nanoparticles in film in the area of 200 × 200 nm with 4 nanoparticles of reference and (b) 3D view of magnetic domains in the 4 nanoparticles observed as islands.

### 3.3. MFM analysis

The topography and magnetic domains of the ZnTe:Cr film grown on glass substrate were observed at room temperature in the remanence magnetization state and the results are shown in Fig. 4(a and b). The average size of the particle in the ZnTe:Cr surface was calculated as 45 nm from AFM analysis. In these nanoparticles, MFM analysis was carried out to scan the magnetic domain distribution over the film. Fig. 5a shows MFM image in a selected area of magnetic interactions. The measurements allowed observing magnetic domain of 4 nm at high resolution. The magnetic interaction on the boundary and cores of nanoparticles showed that the magnetic domains diminished from the core to the boundaries indicating the non-uniformity of the domains.

### 3.4. M–H curve

Room temperature magnetic moment ($M$) data were recorded by varying the magnetic field ($H$) from 0 to 7000 Oe using SQUID magnetometer. Fig. 6 shows the measurement curve, after

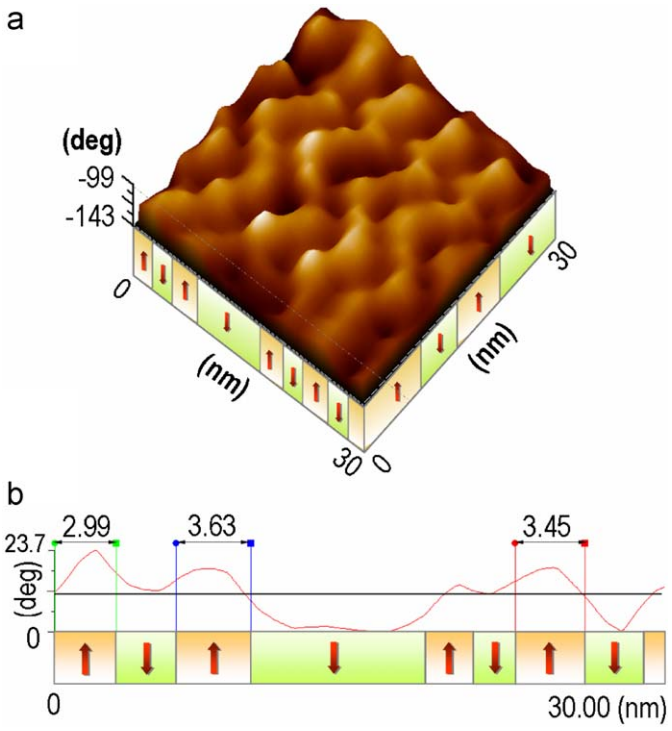


**Fig. 5.** (a and b). Ferromagnetic multi domains of ZnTe:Cr film grown on glass substrate. (a) Domains measured over one surface of $30 \times 30$ nm from the particle 2 indicated in the Fig. 2b. The domains below of 3D image show bright zones which correspond to positive charge (↑) and dark zones indicates a negative charge (↓) and (b) Profile of magnetic domains in cross section correspond to 4 nm.

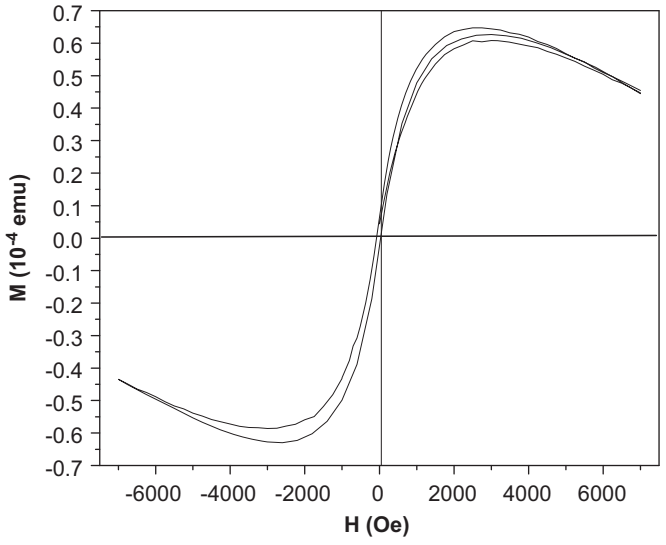


**Fig. 6.** Magnetic moment vs. magnetic field plot of ZnTe:Cr film grown on glass substrate. Diamagnetic contribution from the substrate is subtracted. The diamagnetic contribution from ZnTe host lattice was observed in the higher field region.

subtracting the diamagnetic contribution from the glass substrate. From this magnetic moment data, we obtained the values of coercive field ($H_c$) and remanence magnetic moment ($M_r$) as 48 Oe and $4.3 \times 10^{-6}$ emu, respectively. The calculated coercivity value indicates that the observed hysteresis behavior is ferromagnetic.

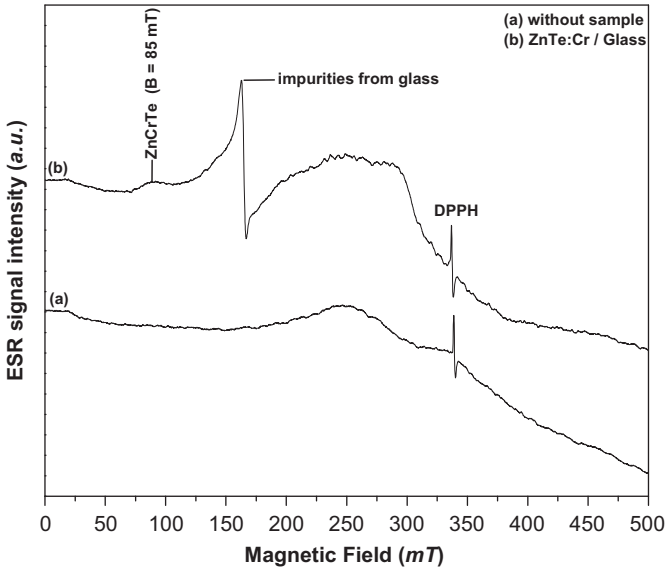


**Fig. 7.** (a–b). The X-band ESR spectra measured (a) in the absence of ZnTe:Cr/glass and (b) in the presence of ZnTe:Cr film grown on glass substrate at 300 K.

### 3.5. ESR spectra

The advantage of ESR spectroscopy is its great sensitivity to the microscopic environment of the unpaired electron/free radical and is a tool to determine the valence state from which the origin of the magnetic moment from the ZnTe:Cr film can be inferred. Chromium enters the ZnTe lattice substitutionally for the divalent cation and is expected to be in the $Cr^{2+}$ valence state. Fig. 7(a and b) display the room temperature ESR profiles measured without sample and measured for the ZnTe:Cr film grown on glass substrate. The spectra of the ZnTe:Cr film shows a weak signal at a magnetic field of 85 mT corresponding to the ZnCrTe phase. In addition we observed a strong sharp signal at $B = 163$ mT which is due to the presence of impurities in the glass substrate [19]. Another sharp signal at $B = 335.3$ mT is due to the DPPH (2,2-diphenyl-1-picrylhydrazyl) free radical. The ESR spectrum of the $I = 0$ chromium isotopes can be analyzed from the following axial spin Hamiltonian:

$$H = g_{\parallel}\beta H_{\parallel} + g_{\perp}\beta H_{\perp}$$

The calculated value of $g_{\parallel} = 7.90$ in the Zeeman interaction term is found at $B = 85$ mT, which is close to the value 7.92 for $Cr^{2+}$ ion in ZnTe crystal as reported elsewhere [20]. As the calculated $g_{||}$ is similar to earlier reported value, it is assigned to isolated $Cr^{2+}$ ions substitutionally incorporated in the zinc lattice site with the valence state of +2.

According to the XRD result we have two ferromagnetic phases in our sample, such as a major ZnCrTe and a tiny CrTe and therefore these two phases might be the origin of the ferromagnetic behavior. However, our room temperature ESR spectra showed an evidence for $Cr^{2+}$ ions substitutionally replaced Zn position. Since the Cr valence is identical for ZnCrTe and CrTe phases, any ferromagnetic property must be from the 2+ state of chromium.

### 3.6. Magneto-optical study

To determine the exact nature of the ferromagnetic behavior we conducted MCD analysis on our as-prepared sample. MCD measures the difference between the absorption of left and right

circularly polarized light. In general, this study will be useful to understand the sp–d exchange interactions and to determine the origin of ferromagnetism. Since the sp–d exchange interactions induce a spin-dependent modification in the host semiconductor band structure, the Zeeman splitting and therefore a sizable MCD signal is expected in dilute magnetic semiconductors. It sensitively detects Zeeman splitting energy ($E$) by measuring the difference between the absorptions for left- and right-circular polarizations, and can be expressed as [21]

$$\mathrm{MCD} = -\frac{45}{\pi}\Delta E\frac{dk}{dE}$$

where $k$ is the optical absorption coefficient and $E$ the photon energy. The above equation shows that the MCD is also proportional to $dk/dE$, which is prominently large around the critical points (CPs) of the band structure in general. Therefore, the MCD is enhanced around the CPs as well. Since each material has its own CP energies reflecting its band structure, we can identify which material is responsible for the observed MCD from its spectral shape.

MCD measurements have been performed on ZnTe and ZnTe:Cr films grown on glass substrate at $T = 6$ K and at a magnetic field of 1 T which was applied perpendicular to the films. The results are shown in Fig. 8(a and b). Our MCD spectrum recorded of the ZnTe film shows signals at photon energies of 2.12, 3.7 and 4.1 eV which are the critical points of ZnTe band structure and reflected $\Gamma$ (2.12 eV) and $L$ (3.7 and 4.1 eV) CPs of ZnTe. A similar measurement of the ZnTe:Cr film is also shown with relatively stronger signals at photon energies 2.12, 3.7 and 4.1 eV reflecting the band structure of ZnTe:Cr shares with ZnTe [10,11]. Since the $\Gamma$ (2.12 eV) CPs are

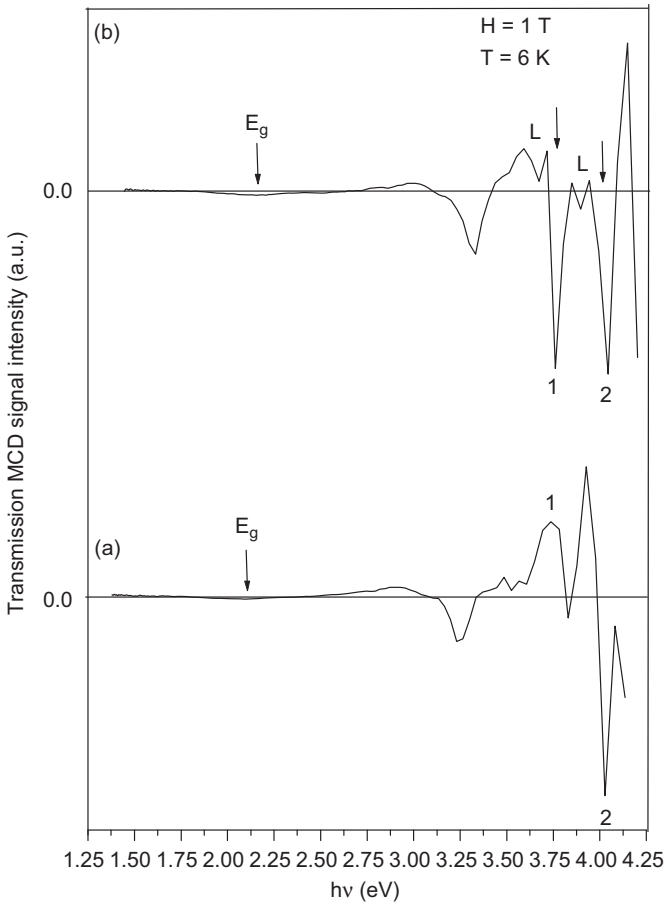


**Fig. 8.** (a–b). Transmission MCD spectra of (a) ZnTe and (b) ZnTe:Cr films recorded at a temperature of 6 K with magnetic field ($H$) = 1 T perpendicular to film plane.

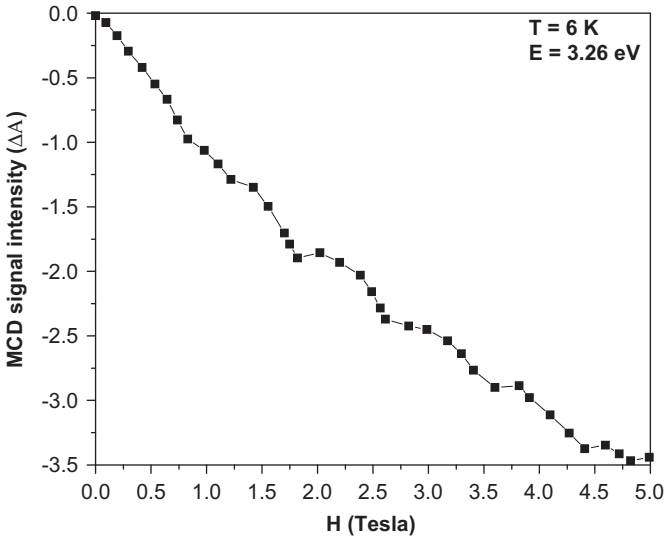


**Fig. 9.** Magnetic field dependence of the transmission MCD intensity ($\Delta A$) recorded at 6 K with a photon energy of 3.26 eV.

exactly the same for ZnTe and ZnTe:Cr films, it is believed that the band gap energy is the same in both the material.

In addition, the polarity of the MCD peak of ZnTe:Cr film at $L$ (3.7 eV) CP is strongly negative and it differs from positive MCD signal of ZnTe [22,23]. This characteristic MCD signal reflects the opposing polarities of the Zeeman splittings at photon energy $L$ (3.7 eV) CP of ZnTe and ZnTe:Cr films. ZnTe:Cr film is therefore confirmed to have the ZnCrTe DMS phase.

Besides to these $\Gamma$-CP and $L$-CPs, a stronger and weak signal was observed from each film at photon energy of 3.26 eV. We believe that this unusual signal must originate from the magnetic impurities from the glass substrate. Since the magnetic effect from glass substrate was subtracted, the contribution from glass substrate to our hysteresis behavior is zero. To determine the type of magnetic impurity we conducted MCD analysis at photon energy of 3.26 eV as a function of magnetic field at 6 K. The result is shown in Fig. 9. Interestingly we observed a diamagnetic effect at this photon energy. It means that the diamagnetic impurity from glass substrate is expected to be the reason for the observed signal at 3.26 eV. From the observed MCD spectra, it is clear that we did not observe any signal reflecting the impurity phase other than ZnCrTe phase from ZnTe:Cr film. It means the origin of ferromagnetic behavior is from ZnCrTe phase.

## 4. Summary and conclusion

ZnTe:Cr film was prepared by thermal evaporation method onto glass substrates. XRD analysis has shown the poor crystallinity along with ZnCrTe phase. MFM investigation has shown a non-uniformity in the magnetic domains. Our SQUID measurement has shown room temperature ferromagnetic nature irrespective of the non-uniformity of magnetic domains in ZeTe:Cr film. ESR spectra revealed the presence of Cr with valence state of +2. The opposite sign of the MCD at the $L$ (3.7 eV) CP of ZnTe and ZnTe:Cr films confirmed the ZnCrTe contribution to the ferromagnetic behavior.

## Acknowledgments

We have a very special acknowledgement to C. Flores-Morales from Instituto de Investigaciones en Materiales, IIM-UNAM by his technical support in AFM characterization.

One of the authors, D. Soundararajan is also thankful to Bharathiar University for the award of University Research Fellowship (URF).

## References

[1] H. Ohno, A. Shen, F. Matsukura, A. Oiwa, A. Endo, S. Katsumoto, Y. Iye, Appl. Phys. Lett. 69 (1996) 363.
[2] H. Munekata, H. Ohno, R.R. Ruf, R.J. Gambino, L.L. Chang, J. Cryst. Growth 111 (1991) 1011.
[3] L.M. Sandrastskii, P. Bruno, J. Phys.: Condens. Matter 15 (2003) L585.
[4] H. Katayama-Yoshida, K. Sato, Jpn. J. Appl. Phy. B. 39 (2000) L555.
[5] M. Imamura, A. Okada, T. Yamaguchi, J. Appl. Phys. 99 (2006) 08M706.
[6] K. Sato, H. Katayama-Yoshida, Semicond. Sci. Technol. 17 (2002) 367.
[7] K. Ando, H. Saito, V. Zayets, M.C. Debnath, J. Phys. Condens. Matter 15 (2003) R1583.
[8] K. Ando, H. Saito, Z. Jin, T. Fukumura, M. Kawasaki, Y. Matsumoto, H. Komuma, J. Appl. Phys. 78 (2001) 2700.
[9] X.G. Guo, J.C. Cao, X.S. Chen, W. Lu, Solid State Commun. 138 (2006) 275.
[10] H. Saito, V. Zayets, S. Yamagata, K. Ando, Phys. Rev. Lett. 90 (2003) 07202.
[11] H. Saito, V. Zayets, S. Yamagata, K. Ando, J. Appl. Phys. 93 (2003) 6796.
[12] H. Saito, W. Zaets, S. Yamagata, Y. Suzuki, K. Ando, Phys. Rev. Lett. 91 (2002) 8085.
[13] K.S. Akram, Z. Ali, A. Maqsood, Appl. Surf. Sci. 143 (1999) 39.
[14] N. Ozaki, N. Nishzawa, S. Marcet, S. Kuroda, O. Eryu, K. Takita, Phys. Rev. Lett. 97 (2006) 037201.
[15] S. Kuroda, N. Ozaki, N. Nishizawa, T. Kumekawa, S. Marcet, K. Takita, Sci. Technol. Adv. Mater. 6 (2005) 558.
[16] JCPDS, X-ray powder diffraction file, Joint Committee for Powder Diffraction Standards.
[17] H. Ye, Q. Zhang, S. Saito, B. Jeyadevan, K. Tohji, M. Tsunoda, J. Appl. Phys. 93 (2003) 6856.
[18] C.D. Wagner, W.M. Riggs, L.E. Davis, J.F. Moulder, C.E. Muielenberg, in: Handbook of X-ray Photoelectron Spectroscopy, Physical Electronics Industries, Eden Prairie, MN, 1976.
[19] M. Diaconu, H. Schmidt, A. Poppl, R. Bottcher, J. Hoentsch, A. Rahm, H. Hochmuth, M. Lorenz, M. Grundmann, Superlattices Microstruct. 38 (2005) 413.
[20] J.T. Vallin, G.A. Slack, S. Roberts, A.E. Hughes, J. Phys. Rev. B. 2 (1970) 4313.
[21] K. Ando, Appl. Phys. Lett. 82 (2003) 100.
[22] K. Ando, Magneto-optics, in: S. Sugano, N. Kojima (Eds.), Springer Series in Solid-State Science, Vol. 128, Springer, Berlin, 2000, p. 211.
[23] K. Ando, A. Twardowski, in: M. Scheffer, Zimmermann (Eds.), Proceedings of the 23rd International conference on Physics of Semiconductors, Berlin. 1996, World Scientific, Singapore, 1996, p. 285.